Tellus (2002), 54B, 110–126
Printed in UK. All rights reserved

TELLUS
ISSN 0280–6509

Tropospheric carbon dioxide concentrations at a northern boreal site in Finland: basic variations and source areas

By T. AALTO[1]*, J. HATAKKA[1], J. PAATERO[1], J.-P. TUOVINEN[1], M. AURELA[1], T. LAURILA[1], K. HOLMÉN[2], N. TRIVETT[3] and Y. VIISANEN[1], [1]*Finnish Meteorological Institute, Air Quality Research, Sahaajankatu 20E, FIN-00810 Helsinki, Finland;* [2]*Department of Meteorology, Arrhenius Laboratory, Stockholm University, S-106 91, Stockholm, Sweden;* [3]*Retired, earlier in Air Quality Measurements and Analysis Research Division, Atmospheric Environment Service, Environment Canada, 4905 Dufferin Street, Downsview, Ontario M3H 5T4, Canada*

(Manuscript received 12 March 2001; in final form 17 December 2001)

ABSTRACT

Diurnal and annual variations of CO_2, O_3, SO_2, black carbon and condensation nuclei and their source areas were studied by utilizing air parcel trajectories and tropospheric concentration measurements at a boreal GAW site in Pallas, Finland. The average growth trend of CO_2 was about 2.5 ppm yr^{-1} according to a 4-yr measurement period starting in October 1996. The annual cycle of CO_2 showed concentration difference of about 19 ppm between the summer minimum and winter maximum. The diurnal cycle was most pronounced during July and August. The variation between daily minimum and maximum was about 5 ppm. There was a diurnal cycle in aerosol concentrations during spring and summer. Diurnal variation in ozone concentrations was weak. According to trajectory analysis the site was equally affected by continental and marine air masses. During summer the contribution of continental air increased, although the southernmost influences decreased. During daytime in summer the source areas of CO_2 were mainly located in the northern parts of the Central Europe, while during winter the sources were more evenly distributed. Ozone showed similar source areas during summer, while during winter, unlike CO_2, high concentrations were observed in air arriving from the sea. Sulfur dioxide sources were more northern (Kola peninsula and further east) and CO_2 sources west-weighted in comparison to sources of black carbon. Source areas of black carbon were similar to source areas of aerosols during winter. Aerosol source area distributions showed signs of marine sources during spring and summer.

1. Introduction

Worldwide measurements have shown that the tropospheric CO_2 concentrations increase continuously. The rate of growth has been accelerating during the last decades together with increased burdening of atmosphere with anthropogenic CO_2 emissions (IPCC, 2001). However, significant inter-annual and inter-latitudinal variability has been observed (e.g. Conway et al., 1994; Keeling, 1995).

Human-induced changes in atmospheric CO_2 will hopefully be controlled through steps firstly introduced in the Kyoto protocol (see http://www.unfccc.de/). Follow-up of the fulfillment of the agreement and the role of natural changes requires continuous monitoring of the world CO_2 pulse. The existing network of measurement stations is comprehensive in marine locations, but much sparser in continental areas, where regional effects often dominate and the back-

* Corresponding author.
e-mail: tuula.aalto@fmi.fi

ground mixing ratio of CO_2 is difficult to distinguish from the local pollution. The number of stations should be increased in order to get a reliable estimate of the large-scale CO_2 balance (Gloor et al., 1999).

Measurements of CO_2 are utilized in estimates of the global carbon budget. There exists evidence of a large northern hemisphere terrestrial CO_2 sink (Ciais et al., 1995). The estimates of the continent having largest contribution to the sink vary from North America (Fan et al, 1998) to North Asia (Bousquet et al., 1999), but more measurements of atmospheric CO_2 are required over the continents throughout the world to verify these results (Fan et al., 1998). These points greatly increase the interest in measuring CO_2 concentrations over continental areas covered by boreal forests, which may have a significant effect on the global carbon balance (Bonan et al., 1995). Furthermore, it is necessary to study CO_2 in a wider context including other species because their partly similar sink/source patterns may also yield information about CO_2.

In this study we present results of a 4-yr measurement period for CO_2 at a WMO GAW (Global Atmosphere Watch — Programme of the World Meteorological Organization) boreal site in Northern Finland. The source areas for high CO_2 in winter and summer are determined and discussed together with corresponding analysis for black carbon, aerosols, ozone and sulfur dioxide. Results are compared with time series from other stations in Arctic and in European midlatitudes.

2. Materials and methods

2.1. Site

Measurements were made in Pallas-Ounastunturi National Park, locally and regionally characterized with a very limited number of pollution sources. The population density on the scale of hundreds of kilometres is less than 2 persons km^{-2}, and the nearest centre of population, Muonio, with 2500 inhabitants, is located at 19 km distance from the measuring site.

The Pallas region is located near the northern limit of the boreal zone. The mean temperature over the year is $-1.6\,^{\circ}C$, but during winter the temperature can drop below $-30\,^{\circ}C$, and during the summer it can rise above $20\,^{\circ}C$. The ground is covered with snow from October to May. The sun is continuously below the horizon from 9 December to 3 January and above the horizon from 26 May to 18 July (the site lies above the Arctic Circle). Wind direction in Pallas is dominantly southwestern during autumn and winter and eastern during spring and summer.

CO_2 is measured at the top of Sammaltunturi (67°58′N, 24°07′E), which is a fjeld (arctic hill) located about 300 m above surrounding terrain and 560 m above sea level (a.s.l.). The top of the fjeld is treeless, and the sparse vegetation consists mainly of mosses and lichens. The treeline is about 100 m below the station. The forest consists of mixed species, mainly Scots pine (*Pinus sylvestris*), Norway spruce (*Picea abies*) and downy birch (*Betula pubescens*). Wetland areas and lakes can also be found at a few kilometres distance. Sammaltunturi belongs to a chain of fjelds extending from south to north, the highest top reaching 800 m a.s.l. There are measuring stations situated at the top of Laukukero (68°04′N, 24°02′E, 765 m a.s.l.), Matorova (68°00′N, 24°14′E, 340 m a.s.l.), Kenttärova (67°58′N, 24°14′E, 330 m a.s.l), and near lake Pallasjärvi (68°01′N, 24°10′E, 303 m a.s.l.) all within 10 km distance of Sammaltunturi.

2.2. Measurements

Continuous CO_2 measurements at Pallas were started in October 1996 by the Finnish Meteorological Institute (FMI) in cooperation with the Air Quality Research Branch of the Atmospheric Environment Service, Environment Canada (AES), who provided the instrumentation and calibration gases. The analyzer system was replaced with a new construction in spring 1998, and calibration gases were now calibrated against the WMO/CCL standards by the Department of Meteorology, Stockholm University, Sweden (MISU). Since summer 2000 FMI has used its own set of WMO/CCL standards for calibration.

Carbon dioxide is measured as a mean of 1-min sampling 12 times per hour with a LiCor NDIR infrared gas analyzer using one reference gas with 318 ppm CO_2 and three calibration gases with CO_2 concentrations of about 338, 358 and 378 ppm CO_2. These working standard concentrations are measured against WMO/CCL primary standards once every 3 months. The deviation has

always been smaller than 0.1 ppm. The sample is collected through heated stainless-steel tubing at about 7 m above ground level. Heating prevents frost formation in the inlet. The residence time inside the tubing is <2 s.

A number of other species are also measured at Pallas (Table 1). Measurements requiring more attention are concentrated on Sammaltunturi (continuous measurements of gas concentrations and CO_2 flask sampling) and Matorova (filter sampling). Sites at Laukukero and Pallasjärvi are equipped with automatic weather stations.

Carbon dioxide fluxes to the surrounding forest were measured at Kenttärova during 16–27 July 1998 by the eddy covariance method. The canopy height at the site was about 13 m, and the fluxes were measured from a mast at 18 m using an IR absorption-based analyzer (LiCor LI-6262) and a three-dimensional acoustic anemometer (ATI SWS-211). A detailed description of the measurement set-up is presented in Rinne et al. (2000). The eddy covariance measurement also offered information about the CO_2 concentration near the forest terrain, although the results were not as accurate as at Sammaltunturi (more than 10-fold difference in precision) because the equipment was

Table 1. *Measurement scheme at Pallas region*

Species	Instrument or measurement method	Sampling frequency	Location
Surface O_3	Two Dasibi ozone meters	Continuous	S
SO_2	Thermo Environmental Instruments 43 S	Continuous	S
CO_2, N_2O, CH_4	Glass flask samples	1/wk	S
CO_2	Li-Cor Infra-red gas analyzer	Continuous	S
VOCs	850-ml stainless steel flasks	2/wk	S
Sulfate	Filter	Daily	M
SO_2	Impregnated filter	Daily	M
Nitrate + nitric acid	Filter + Impregnated filter	Daily	M
Ammonia + ammonia	Impregnated filter	Daily	M
Heavy metals	Filter	Weekly	M
Mercury. particulate	Filter (with IVL)	Weekly	M
Mercury, gaseous	Goldtrap (with IVL)	2 d/wk	M
POPs	Filter + polyurethane foam (with IVL)	1 wk/month	M
Condensation nuclei			
$D_a > 10$ nm	TSI CPC model 3010	Continuous	S
$D_a > 0.3$ μm	TSI Laser Particle Counter	Continuous	S
Particle size distribution 10–450 nm	DMPS	Continuous	S,M
Black carbon (BC)	Aethalometer (Magee Scientific)	Continuous	S
Radon-222	Aerosol beta activity measurement	Continuous	S,M
Radon-222	Accumulation chamber, alfa counting (with EML)	Continuous	S
Dose rate	Eberline ionisation chamber	Continuous	M
Electrical conductivity	Gerdier-cylinder	Continuous	M
Surface weather parameters	Vaisala MILOS500 + sensors	Continuous	S,M,L,P
Solar radiation			
Global irradiance	Kipp & Zonen pyranometer CM11	Continuous	S
$J(NO_2)$	Radiometer (Meteoroloogie Consult GmbH)	Continuous	S
Precipitation chemistry			
pH, conductivity, major ions	Bulk collector	Weekly	M
Heavy metals	Bulk collector	Monthly	M
Mercury	Bulk collector (with IVL)	Monthly	M
POPs	Bulk collector + polyurethane foam (with IVL)	1 wk/month	M

Location: S, Sammaltunturi; M, Matorova; L, Laukukero; P, Pallasjärvi. IVL, Swedish Environmental Institute, Gothenburg, Sweden. EML, Environmental Measurements Laboratory, DOE, USA.

designed for accurate flux measurements instead of absolute concentration measurements.

2.3. *Trajectory analysis*

Finding the most important sources for measured species is usually a difficult task in a variable environment retaining diverse sinks and sources in continental vegetation, populated areas and marine regions. One approach for source analysis is to combine a calculated path of an air parcel, trajectory, to the observed concentration at the moment of arrival of the parcel to the site and determine approximate locations of sources from a representative set of observations (e.g. Stohl, 1996; 1998).

In this work trajectory studies were performed for several measured species. Two sets of trajectories were used, one generated by FMI and the other by AES. AES trajectories were calculated using the isobaric model of Olson et al. (1978) and utilizing wind fields from the Canadian Weather Forecast model. Trajectories were calculated for arrival times of 00:00 UTC, 06:00 UTC, 12:00 UTC and 18:00 UTC (= local standard time −2 h) and arrival levels of 925 hPa and 850 hPa. Path and height of the air parcel were calculated backwards in time every 6 hours for 5 days. The set covered years from 1996 to 1998. FMI trajectories were generated using an operational model TRADOS (Pöllänen et al., 1997) which utilizes numerical meteorological data from a Finnish version of the weather forecast model HIRLAM (High Resolution Limited Area Model). Trajectories were calculated for the same arrival times as AES at levels 920, 955 and 965 hPa. Path and height of the trajectory were calculated once every hour and 4 d backward in time during the years 1997–1999.

Concentration charts were calculated by combining measured concentrations and air parcel trajectories (see Seibert et al., 1994). The concentration data sets were normally or log-normally distributed depending on the species. According to the study material CO_2 and O_3 appeared to be normally distributed and condensation nuclei, black carbon and SO_2 log-normally distributed. An arithmetic mean concentration was calculated for every hour (measurements were usually made 12 times during 1 h) when the data were normally distributed. A geometric mean was calculated when the data were log-normally distributed. The resulting hourly mean concentration was assigned to each $1^\circ \times 1^\circ$ area crossed by the trajectory before arriving at Pallas during the corresponding 1-h time window. The procedure was repeated for the whole trajectory set. As a result, most $1^\circ \times 1^\circ$ grid cells were crossed by several trajectories and had several concentration values assigned to them. The values were averaged separately for each grid cell and then redistributed in an iterative procedure that assigns the concentration along the corresponding trajectory in an unequal fashion. The high emission regions eventually end up having the highest concentrations in relation to the original, observed concentration and the new mean concentration along the trajectory. The iteration ends when new redistributions do not change the result, and the final concentration field is smoothed. The redistribution-smoothing method was developed by Stohl (1996), and his procedures were utilized in preparing the concentration distributions for this work. The redistribution method may not always be suitable for species which go through non-linear chemical processes during transport. For example, according to Stohl (1998) wet deposition processes may have a negative impact on the aerosol source area results. However, Stohl (1996) has been using the method succesfully for particulate sulfate, and Virkkula et al. (1998) also used the method for SO_2 and aerosols with good results. Since the current results are rather stable for all short-lived species and agree with emission charts, there is no apparent reason why the method should not be used here. Non-linear processes may, however, reduce the quality of the results especially for ozone and aerosols.

One weakness generally associated with the use of trajectories is that the air parcels might have been passing above the boundary layer with no exchange with the surface. Those parts of the trajectory path should be excluded from the source area analysis. In the current work we assume that the problem disappears with a large number of trajectories crossing the same area at different times of the day from different directions. The distribution of the concentration along the trajectory also requires several concentration values per grid cell in order to find out which cells are sources. In order to be included in the concentration chart, each $1^\circ \times 1^\circ$ area was required to be

crossed by at least 10 trajectories, although in some cases only five crossings were required due to limited number of observations. The results were not very sensitive to this parameter. The effect of changing the crossing limit could be seen in practice in the extent of the modelled source area. Limiting the extent of the modelled area also limits the amount of information attainable from the concentration charts: the study can not cover single events of very long-range transport, which might be necessary on the basis of the long atmospheric residence time of CO_2.

We also estimated the relative importance of different source areas by calculating approximate residence times of air parcels in the specified region (Fig. 1). The residence time was obtained by counting the number of incidents in every $1^\circ \times 1^\circ$ area crossed by a trajectory. If the distance between subsequent grid points was greater than one, the gap was filled linearly so that all (probable) crossed grid points on the track of the air parcel were counted. However, the weight of the filled point was decreased in proportion to the number of added points (+endpoint), so that the weighting or relative importance of the whole trajectory remained constant. In essence, if the air parcels moved fast their residence time per grid point was decreased. 4384 trajectories (1996–1998) by AES (925 hPa arrival level) were used, since they extend to 5 d backward in time and use global weather data. For comparison, 1052 trajectories by FMI during the year 1999 were utilized. The 955 hPa level was chosen since it is closest to the level of the measurement site.

3. Results and discussion

3.1. Annual and diurnal cycles of CO_2

Both annual and diurnal sequences of CO_2 were observed at Sammaltunturi (Figs. 2 and 3). CO_2 levels also increased year by year. A growth trend was estimated from the observations by fitting the following equation to the data (see e.g. Tans et al., 1989, and Kahaner et al., 1989):

$$x(t) = x_0 + x_1 t + \sum_k \left[a_k \sin\left(\frac{2\pi t k}{T}\right) + b_k \cos\left(\frac{2\pi t k}{T}\right) \right] \quad (1)$$

where x is the mixing ratio of CO_2 and t is time (if expressed in years then sequence T equals 1). The coefficients to be fitted include constant x_0, growth trend x_1 and coefficients for the harmonic function, a_k and b_k, where $k = 1$–3. The fitting procedure was repeated for daily medians and for a selected dataset where only measurements during 12:00–16:00 LT with wind speed > 2 m s^{-1} were utilized. Standard deviation σ was used for additional classification: data points with distance larger than 3σ from the harmonic curve were deleted. Results were similar for both sets and indicated an average growth trend of 2.5 ppm yr^{-1} (see e.g. http://www.cmdl.noaa.gov/ccgg/figures/

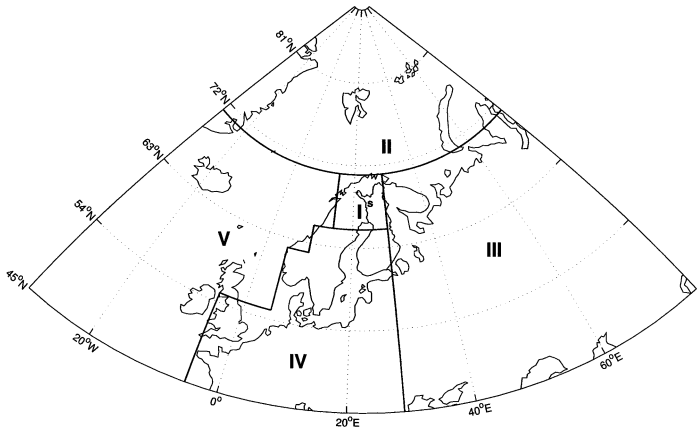

Fig. 1. Schematic representation of source regions for air parcels arriving to Sammaltunturi (location marked with **s**).

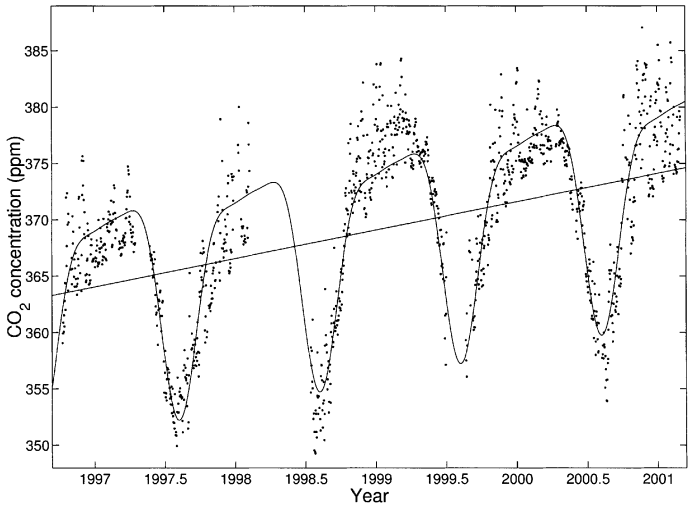

Fig. 2. Time series of CO_2 measured at Sammaltunturi during 1996–2001. Dots refer to daily medians. Curved line is the fit according to eq. (1) and straight line is the linear part of eq. (1), which shows the growth trend.

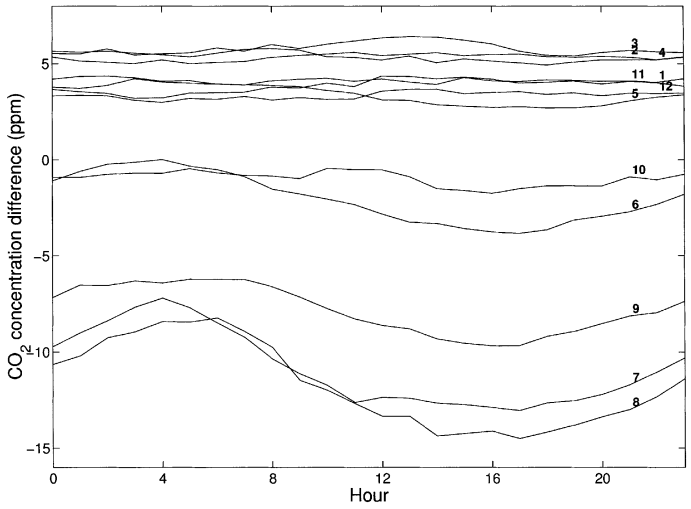

Fig. 3. Averaged diurnal variation of CO_2 according to hourly medians (UTC + 2 h) measured during 1996–2001 at Sammaltunturi. Numbers refer to months. The growth trend had to be removed before averaging, and therefore the *y*-axis is expressed as CO_2 concentration difference rather than CO_2 concentration. The difference is calculated from observed concentration and concentration given by the linear part of the harmonic function [eq. (1)].

figures.html for global results). The annual mean for the year 1999 seemed to be higher than expected from the growth trend. Another possibility is that the growth rate was slightly smaller during the most recent years. It has to be remembered, however, that the study material consisted of only four complete years, and thus definitive conclusions can not yet be made. The concentration difference between the yearly maximum and minimum was about 19 ppm.

The summer minimum at Sammaltunturi covered July and August (Fig. 4), starting roughly one month earlier in comparison to the WMO/GAW stations Ny Ålesund (78°54′N,

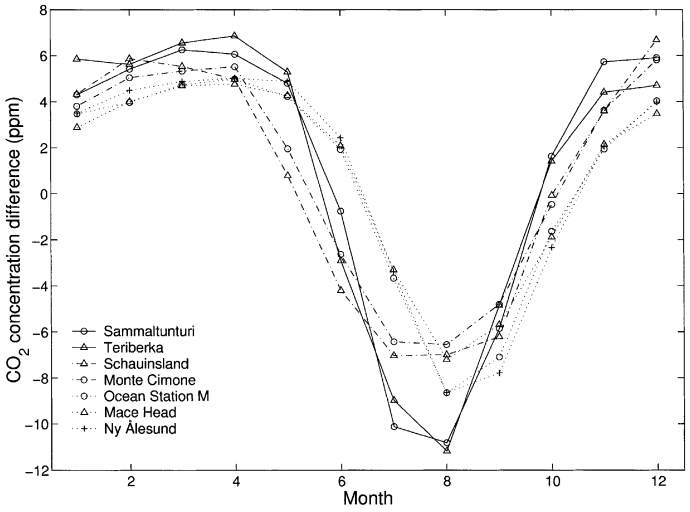

Fig. 4. Averaged seasonal variation of CO_2 according to monthly means at different stations. The concentration difference is the difference between observed concentration and concentration given by a linear function fitted to the data.

11°54′E), Ocean Station 'M' (66°00′N, 2°00′E) and Mace Head (53°19′N, 9°53′W), which are all located in marine Atlantic environment covering a north–south distance of almost 3000 km (data adopted from WMO WDCGG CD-ROM No. 7, Japan Meteorological Agency, Tokyo, also available at http://gaw.kishou.go.jp/wdcgg.html). At Teriberka (69°12′N, 35°06′E), a coastal station in Kola Peninsula, the summer minimum occurred at the same time as in Sammaltunturi, which is at the same latitude. The yearly variation at Sammaltunturi showed some similar features to continental background sites in Germany (Schauinsland, 47°55′N, 7°55′E) and Northern Italy (Monte Cimone, 44°11′ N, 10°42′ E), except that at the southern sites the concentration started to decrease earlier in spring and stayed low for at least one month longer in autumn. Timing of the summer minimum can be attributed to many things. Pallas region experiences a later start to and shorter duration of photosynthetic activity than southern sites, but as source areas are large, timing of the springtime uptake by marine phytoplankton and removal of ice coverage and subsequent strengthening of the CO_2 sink in the sea may also have an effect on concentrations at Pallas. According to Fig. 4, however, the seasonal cycle at Pallas shows more continental features. The cycle is also very smooth in comparison to measurements at sites where regional sources of CO_2 dominate over background (e.g. Deuselbach in Germany; see Levin et al., 1995).

A pronounced and continuous diurnal cycle can usually be observed at Sammaltunturi from June to September. The mean variation between daily minimum and maximum was about 5 ppm at 560 m a.s.l. during July and August (Fig. 3). According to the concentration readings from the eddy covariance system, which was in operation for two weeks in July 1998 (the difference was also 5 ppm at Sammaltunturi during this period), the difference between daily minimum and maximum was about 24 ppm near the surrounding forest at Kenttärova (330 m a.s.l.). The daily variation thus increased with decreasing altitude. The amplitude is mainly affected by photosynthetic and respirational activity in the region and boundary layer dynamics at the site. The local differences in fluxes between the two sites may also affect the result, although the sites are situated close to each other. Comparison with the local flux measurements indicated that the concentration at Sammaltunturi followed the daily development of the sink with a few hours delay. Bakwin et al. (1998) found daily variations of the order of 40 ppm during July at 10–50 m above ground in North American mid-latitudes. The variation decreased below 10 ppm at altitude of about

250 m. The American site characteristics include larger CO_2 fluxes, leading to a larger amplitude in comparison with Pallas region. However, the relative decrease of amplitude with increasing altitude was comparable to the amplitude change between Kenttärova and Sammaltunturi.

The diurnal cycle at Sammaltunturi started to develop about one month later in comparison to Central European WMO/GAW sites in Germany and Northern Italy. The amplitude of the diurnal cycle was very similar to, for example, Monte Cimone (44°11′N; see Colombo et al., 2000) and Schauinsland (47°55′N), sites which are both located at altitudes over 1000 m a.s.l. The diurnal cycle was practically non-existent at the Arctic marine sites Zeppelinfjellet (78°54′N) and Point Barrow (71°19′N), while at Mace Head a small cycle of a few ppm was found from early spring to fall. In comparison to the continental Central European sites the later start in the photosynthetic activity at Pallas can be seen on the development of diurnal cycles and on the delayed, steep concentration decrease towards the summer minimum.

3.2. *Mixing of the boundary layer*

It is important to study the extent of vertical mixing in the boundary layer in order to find out how often the measuring site is coupled with the local surface. The mixing layer usually extends to its highest altitudes during summer afternoons. Temperature soundings at Sodankylä observatory (125 km SE from Pallas) show that during summer afternoons this mixing layer usually extends to 1000–1500 m. This is probably also a valid result for Pallas region, although fjelds may distort the structure of the boundary layer. Weather station readings from different altitudes at Laukukero (765 m), Sammaltunturi (560 m) and Pallasjärvi (303 m) did not usually indicate temperature inversions during the daytime, while during the night (21:00–06:00) inversions were found between Sammaltunturi and Pallasjärvi. The lowest site, Pallasjärvi, thus seemed to be decoupled to some extent from Sammaltunturi and Laukukero during the night. This is also supported by studies with radon-222 (Paatero et al., 1999). Radon is naturally emitted from the ground and it accumulates in the stable, shallow nocturnal mixing layer. During daytime the height of the mixing layer increases and radon is diluted in the larger air volume. At the level of Sammaltunturi no pronounced diurnal cycle of radon was observed, which indicates that the site was above the nocturnal mixing layer. A short pulse of radon was sometimes observed during morning hours, indicating rapid collapse of the inversion. Some of those pulses also coincided with a rise in CO_2 concentration. The long-range transport may contribute to the fact that the pulses were not always simultaneous. Also, the emission rate of radon is low during early spring when the soil is frozen. Vegetation may still produce short-term respiration pulses if the air temperature and irradiance are high enough. In order to study this in detail, springtime eddy covariance measurements would be needed.

3.3. *Source area analysis*

Factors that affect the observed CO_2 concentration at Sammaltunturi include meteorological conditions, gas exchange by land and sea biota, temperature-induced changes in the solubility to sea water and anthropogenic influences. Although the location of Sammaltunturi is not coastal, marine influences are possible due to long-range transport from the Atlantic Ocean or northernmost parts of the Baltic Sea both at distance of 250–350 km. Trajectories can be used to study the role of different source areas.

3.3.1. Characteristic source regions of air parcels. The source regions for Sammaltunturi were roughly categorized as in Fig. 1, and the air parcel residence times in these regions were calculated as explained in Section 2.3. Results for different regions using Canadian trajectories are shown in Table 2. Comparison with the FMI trajectories showed similar results except that the AES 5-d 925 hPa trajectories obviously extended to longer distances. For example, 7.7% of the 925 hPa trajectories passed over areas south of 55°N, while only 5.8% of the 955 hPa trajectories did the same. The difference may also be partly due to different arrival heights. The lower arrival level for the FMI trajectories increases the possibility that the air has been spending a longer time close to the arrival point. The starting points of 925 hPa trajectories were in the average at a distance of 1930 km from Sammaltunturi, but the longest distances were of the order of 6000 km. The mean

Table 2. *Contributions of different regions (see Fig. 1) to path of air parcels arriving to Sammaltunturi*

Region Month	I N. Sca.	II Arctic	III East	IV South	V N. Atl.	II + V Marine	I + III + IV Contin.
1–2	16.5	28.9	12.1	18.8	23.6	52.5	47.5
no I	—	34.7	14.5	22.5	28.3		
3–4	20.1	34.4	16.3	12.8	16.3	50.7	49.3
no I	—	43.1	20.4	16.0	20.5		
5–6	24.5	33.3	13.3	8.54	20.4	53.7	46.3
no I	—	44.1	17.7	11.3	27.0		
7–8	27.6	19.5	19.9	16.3	16.6	36.1	63.9
no I	—	26.9	27.5	22.6	23.0		
9–10	19.8	24.5	17.9	17.2	20.7	45.2	54.8
no I	—	30.5	22.3	21.5	25.8		
11–12	20.4	25.7	14.6	21.1	18.3	44	56
no I	—	32.2	18.3	26.5	23.0		
All	21.5	27.7	15.7	15.8	19.3	47	53
no I	—	35.3	20.0	20.1	24.6		

Numbers refer to percentage of crossings of $1^\circ \times 1^\circ$ squares in a certain region from all crossed squares. N. Sca., Northern Scandinavia; N. Atl., Northern Atlantic; no I, region I excluded.

distance of starting points of 955 hPa trajectories was 1380 km. Different trajectory calculation methods may also lead to different results. Three-dimensional trajectories (FMI) are considered to be more accurate than isobaric trajectories (AES). The uncertainty of the trajectory path also increases with the number of days calculated backwards. The 5-d AES trajectories may thus be more erroneous than 4-d FMI trajectories.

Northern Scandinavia (region I) was a special case, since it was crossed by all trajectories from all regions and thus automatically became the most important source area. The percentages, however, are of some interest, since they provide information about the activity of the air mass movement and thus transit times over the region during the year. The fractions were largest during late spring and summer, indicating slower movement of air parcels and increase of the importance of the nearest, mostly pollutant-free continental region.

The Arctic (north of 71°N) was clearly the region with the highest number of trajectory crossings (Table 2) for a major part of the year. Only during July and August the contributions from East (region III) and Northern Scandinavia were larger. North Atlantic (region V) influences were at maximum during January and February. Residence time in South (region IV) also increased during winter and decreased during summer. Considering south further, the majority of anthropogenic CO_2 emissions are emitted from below 55°N. Trajectory crossings of grid boxes below 55°N represented only about 4% of all crossings during May–August and 8–13.5% of crossings during September–April. When the regions were roughly categorized to marine (Arctic and North Atlantic) and terrestrial (North Scandinavia, East and South), the result was near half-and-half though fraction for continental region was larger during July and August (Table 2). When Northern Scandinavia was excluded the fraction was clearly larger for marine air. These results agree with Hatakka et al. (2001) and Rummukainen et al. (1996) in indicating the Arctic as a major source region of air arriving at Pallas.

3.3.2. Concentration charts. Trajectory-based source area analysis requires a large number of observations in order to achieve plausible results. However, because of the strong seasonality of CO_2 concentration the time periods with comparable concentration ranges are rather short. During spring and autumn study periods of the order of one month are suitable because the source/sink regions and the mean concentration change rapidly, and the concentration chart might be skewed if winds from certain sector dominate during some part of a long study period. Of course, single fluctuations are rather well recognized also

during long study periods, but they are averaged to some extent so that their relative influence decreases. Diurnal variation of CO_2 is strongest during July and August. During these months, at least, it is necessary to consider night and day separately. Same conclusion applies for aerosol and ozone concentrations, where some signs of diurnal cycle were found. A suitable set of months for source area analysis varied among species. For example, CO_2 experienced a strong yearly cycle and relatively small fluctuations (in comparison to e.g. SO_2). Thus suitable CO_2 data set for 'summer' covered only July and August. Moreover, only trajectory arrivals at 08LT and 14LT were utilized due to the diurnal variation in CO_2 concentration. Night-time arrivals could also be used, but on the other hand anthropogenic sources are more easily detectable from the daytime observations when the local background concentration is not so high.

During winter the sources of CO_2 from heating-induced fossil fuel burning are distributed more evenly and there are fewer sinks than during summer. Ice covers the North Atlantic until Greenland Sea. Terrestrial vegetation is at dormancy, although soil respiration continues at moderate level according to several ecosystem flux measurements (e.g. Markkanen et al., 2000; Aurela et al., 2001; see also Laurila et al., 2001). This corresponds especially to the non-permafrost sites, which form the majority also at Northern Scandinavia. According to the current study the distribution of CO_2 was indeed quite uniform above land during winter (Fig. 5). The 'winter-type' source area distribution was fully developed at November and lasted until April. During summer the photosynthetic sink is strong in the large forested regions of Scandinavia and Northern Russia. The sea also acts as a sink due to the photochemical activity of the phytoplankton and cooling of surface waters brought to north by the North Atlantic Current. Decreasing seawater temperature forces more CO_2 to be dissolved in water in order to re-establish the equilibrium conditions [see e.g. Engardt and Holmén (1999) for CO_2 studies in marine arctic conditions]. According to the current study low CO_2 concentrations were observed above sparsely populated regions during summer at daytime and the highest concentrations seemed to enter in air masses from southwestern direction (Fig. 5). High concentrations in air masses from northern parts of the Central Europe agree with the fossil fuel source inventory by Andres et al. (1996). Of course, exact source areas are impossible to identify here, and it is more justified to only indicate the direction where high concentrations are observed in the limits of the study region. High concentrations were also occasionally observed above the marine area in the NW corner of the study region, which might indicate transport from the North American continent. This is in agreement with earlier studies concerning ozone and lead-210 (Rummukainen et al., 1996; Paatero and Hatakka, 2000). Southern Sweden and Southern Finland can also be pointed out as moderate source regions.

Ozone showed some similar features to CO_2. Summertime high concentrations were produced in the SW sector (Fig. 6). In winter the concentration of ozone was slightly higher above the sea, which was opposite to CO_2 results (Fig. 5). CO_2 and precursors for ozone (nitrogen oxides and volatile organic compounds) are both produced in populated and industrialized regions (Logan, 1985; Andres et al., 1999; see also Laurila and Hakola, 1996; Laurila, 1999). Both are deposited to vegetation during growing season. The ozone-producing photochemical reactions and deposition sink strength are suppressed during winter as well as the photosynthetic sink of CO_2. However, the ozone-destroying reactions continue in the dark, and the pollutant emissions may create an ozone sink during winter (Fig. 6) as well as they create a source during summer days. Ozone chemistry is, however, rather complex, and the lifetime varies significantly according to site (urban/background), season, altitude and latitude. At a northern background site it is probably several days during summer (Seinfeld and Pandis, 1998). In comparison to CO_2 it is more difficult to say where the high concentration was actually formed and how much was lost on the way, which can perhaps be seen in the somewhat more smeared concentration chart. The weak diurnal variation in observed concentration is typically due to the site being located far from large population centers where precursors of ozone are produced. The variation is lost in large-scale mixing and transport of air masses (see e.g. Logan, 1985).

Black carbon particles are produced mainly by fossil fuel and biomass burning (Cooke and

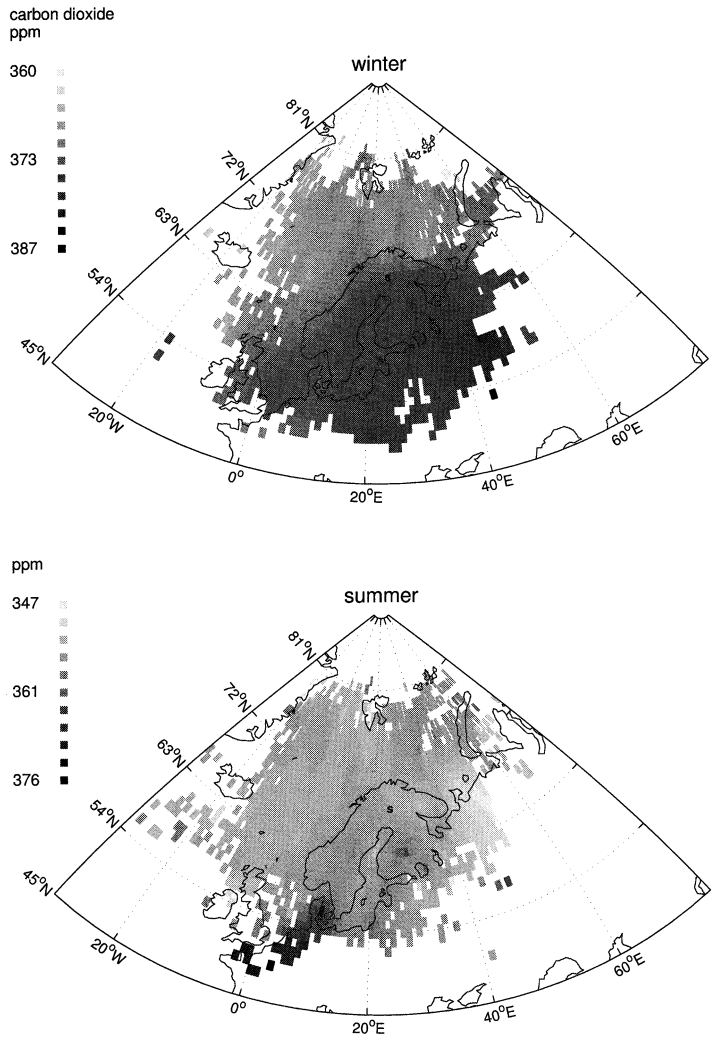

Fig. 5. Carbon dioxide concentration distributions estimated using an air parcel trajectory set to Sammaltunturi (location marked with **s**). Summer months refer to July–August and winter to November–March.

Wilson, 1996). The role of biomass burning (e.g. forest fires) is minor in Northern Europe. As anthropogenic CO_2 is produced mainly by fossil-fuel burning, cement production and gas flaring (Andres et al., 1996), similar source areas are expected. A contrasting factor is that the residence time of black carbon in the atmosphere is considered to be only few days, while the residence time of CO_2 is several years. Thus the black carbon observations may suffer from signal loss (like ozone). On the other hand, a few days should be sufficient to bring the air masses containing black carbon to Pallas from the limits of the study area (Central Europe). In practice the observed source area for black carbon was shifted slightly to the east in comparison to CO_2 during summer (Fig. 7), which may be due to the differences between eastern and western technologies in fossil-fuel processing. It may also be possible that more sources of black carbon exist beyond the south-western limit of the study area where the high CO_2 air masses seemed to enter, but they were not observed because the transport time was too long for black carbon. During winter the source

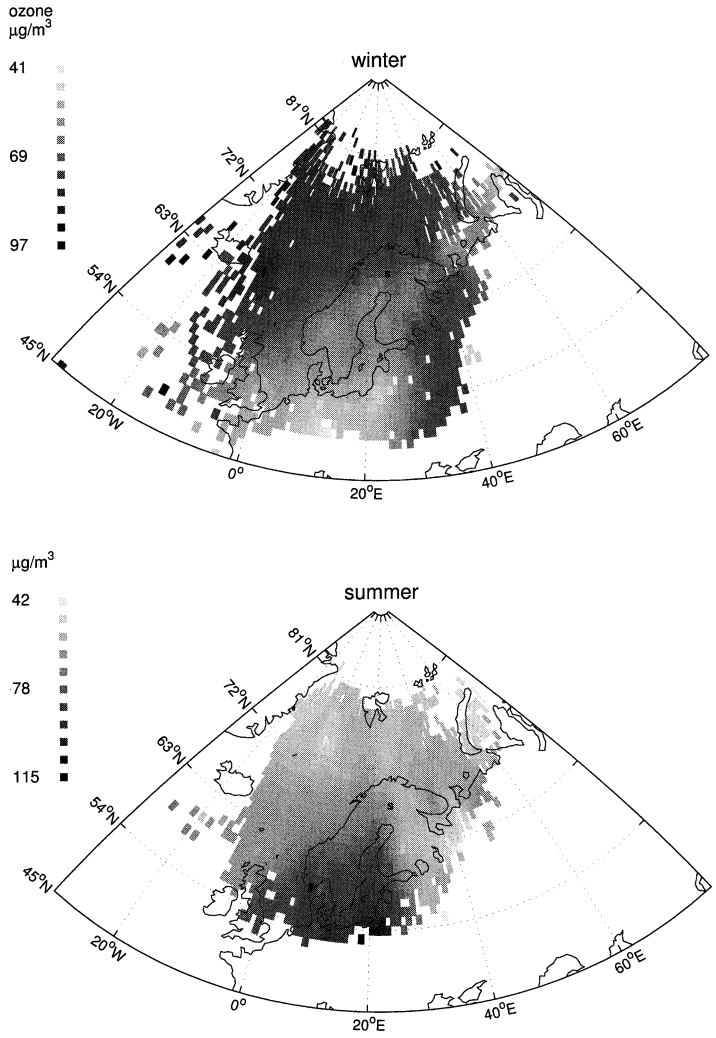

Fig. 6. Ozone concentration distributions estimated using an air parcel trajectory set to Sammaltunturi (location marked with **s**). Summer months refer to June–August and winter to November–February.

area for black carbon extended further to the north and east (Fig. 7), while CO_2 was more evenly distributed.

SO_2 source areas were rather similar throughout the year, but concentration levels were higher during winter, probably due to suppressed gas-to-particle conversion, deposition and vertical mixing (e.g. Rahn et al., 1980; Tuovinen et al., 1993; Ahonen et al., 1997). High concentrations were found in air masses which crossed the Kola Peninsula industrial area (Fig. 8), but the source area extended even further to the east, indicating contributions also from other industrial complexes, possibly the Norilsk area. Similar results were found by Virkkula et al. (1998), who made a source analysis for the Sevettijärvi station, 200 km northeast from Sammaltunturi and only about 60 km west from Nikel (in the Kola industrial area). During summer the CO_2 emissions from these industrial areas were masked by the terrestrial sink in the vicinity, but during winter they may appear as CO_2 sources. For example, Engardt and Holmén (1999) redistributed anthropogenic CO_2 sources in the region according to

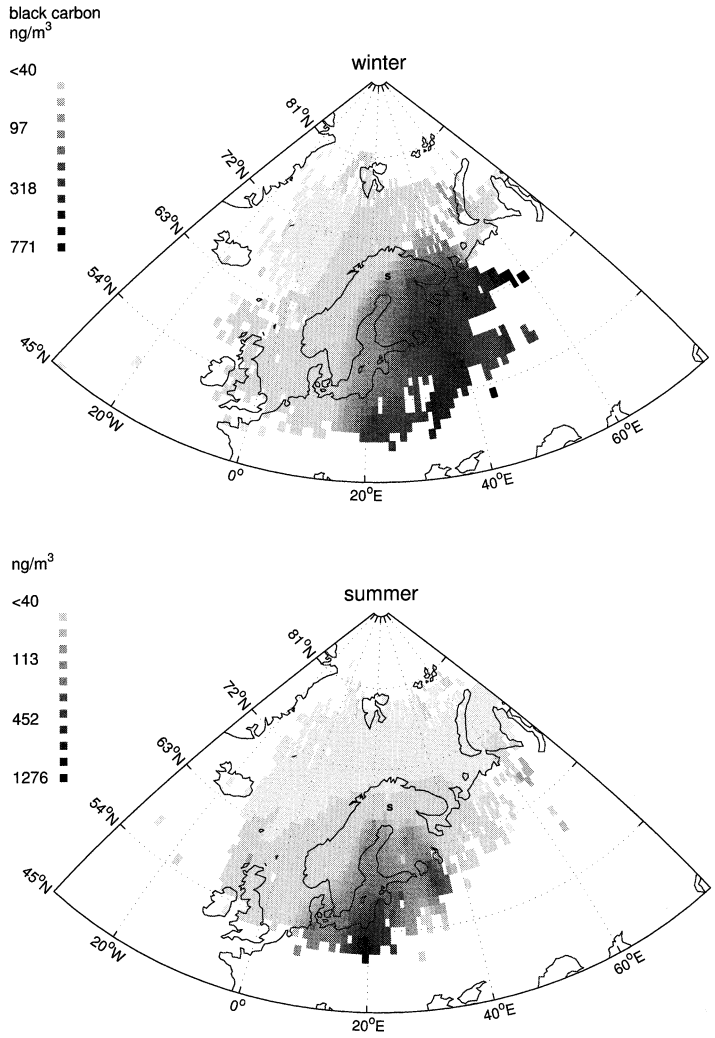

Fig. 7. Black carbon concentration distributions estimated using an air parcel trajectory set to Sammaltunturi (location marked with **s**). Log_{10}-scale. Summer months refer to May–September and winter to November–March.

SO_2 emissions. The lifetime of SO_2 is only of the order of few days. Large sources of SO_2 are, however, rather well known and can easily be detected from the concentration distribution map.

Condensation nuclei (CN) are newly formed particles that may originate from pollutant gases or diverse natural (for example marine DMS or terrestrial VOC) sources (e.g. Seinfeld and Pandis, 1998). Source areas for CN were not very similar to SO_2. In particular, during winter the distribution was more like that of black carbon (Fig. 9). During summer marine locations appeared as a significant source area (Fig. 9). The results by Virkkula et al. (1998) showed a more Kola-concentrated source, which can be expected due to the vicinity of the site. The lifetime of CN is similar to SO_2 and black carbon, usually only of the order of few days. The diverse sources of CN also mix up the distribution pattern in comparison to SO_2, with only a few very large sources. Many natural processes form a sink of CO_2 and source of CN. The more diverse and variable source area for CN can be one indication of the shorter lifetime in comparison to CO_2. CN concentration showed

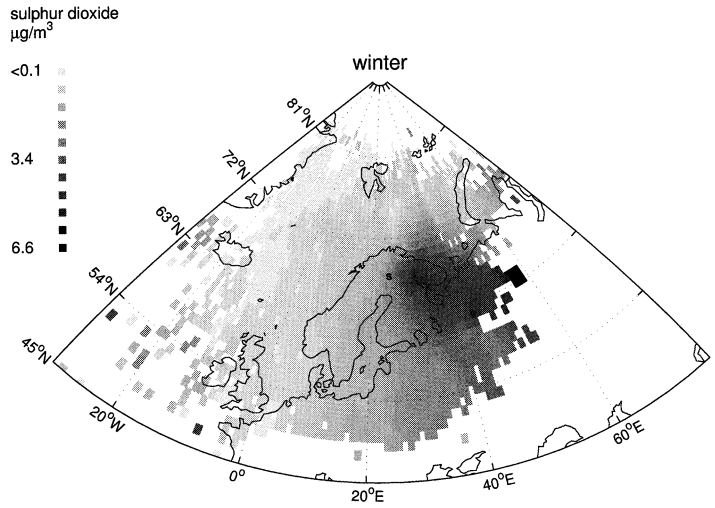

Fig. 8. Sulfur dioxide concentration distributions estimated using an air parcel trajectory set to Sammaltunturi (location marked with **s**). Winter months refer to November–March.

signs of diurnal variation during spring and summer. The cycle was most pronounced in April and May. This was reflected to the source area distributions as recurrent bursts of aerosols in marine regions. Photochemical formation processes are diminished during the night, although night (or dusk) in polar regions is very short during spring and summer. More consistent high concentrations were found in air masses from southern locations, indicating terrestrial sources.

4. Summary and conclusions

Diurnal and annual variability in CO_2 source areas and their relation to other species was studied by utilizing air parcel trajectories and tropospheric concentration measurements at a boreal (subarctic) site. Local influences were obvious during the daytime at summer, when the mixing layer height usually extended to altitudes higher than the site, but during the night the transport from the surface was restrained. However, the site can probably be considered as a background site with a tolerable amount of local influence (i.e. measurements are mostly representative for large and horizontally well-mixed air masses and thus suitable for studies of the global CO_2 balance). The diurnal cycle of radon was practically non-existent at the site, and annual and diurnal cycles of CO_2 were smooth in comparison to regional Central European sites. They were similar to continental background sites in mountainous locations in Europe. Differences were found in the length of the summer minimum and development of the diurnal cycle, which occurred about one month later at Sammaltunturi than at European background sites. The duration of the summer minimum was longer at continental sites. At marine sites the summer minimum usually occurred one month later than at Sammaltunturi.

According to trajectory analysis the source area of CO_2 extended to Scandinavia, Northwestern Russia, Norwegian Sea, Barents Sea and northern parts of Central Europe. Regional characteristics include boreal forest, agricultural land, few industrial areas and marine environments. Most of the source area was sparsely populated, but emissions from large CO_2 and other pollutant sources were detected through long-range transport. Large pollutant sources were located in regions contributing 30–40% on the source area (East and South in Table 2). During most of the time the site was nearly equally affected by marine and continental air masses. The continental residence times were clearly larger only during summer.

During daytime in summer the largest CO_2 concentrations entered in air masses from a southwestern direction, indicating transport from the densely populated and industrialized areas in

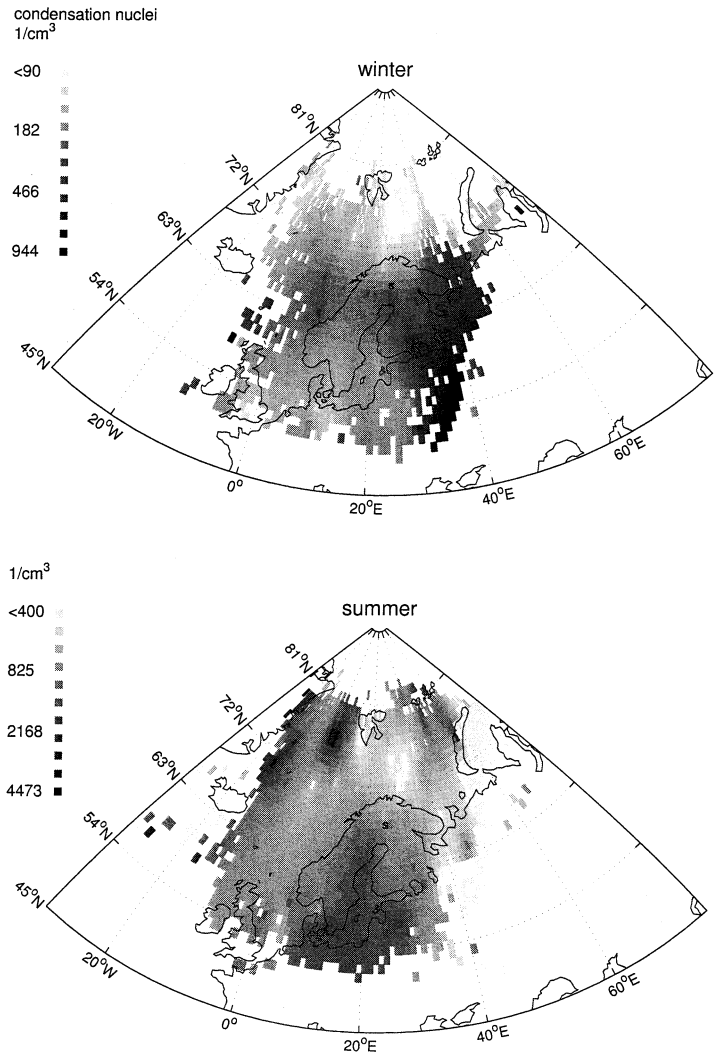

Fig. 9. Condensation nuclei concentration distributions estimated using an air parcel trajectory set to Sammaltunturi (location marked with **s**). Log_{10}-scale. Summer months refer to June–August and winter to November–February.

Central Europe. Wintertime source areas were more uniformly distributed across continental regions due to respiration and decreased CO_2 sink. Low concentrations above the sea in winter may support sources in land or indicate a sink in sea due to solubility in unfrozen waters. This result was opposite to ozone, where low concentrations were found above land during the winter, probably due to a continuing sink in the populated regions. During summer O_3 source areas were similar to those of CO_2. Distribution of high concentrations of black carbon was more eastern than high CO_2 in summer, possibly due to different technological solutions for combustion processes. During winter black carbon emissions extended further to northeast. The fine particle distribution resembled mostly that of black carbon during winter, while during spring and summer marine sources were detected and there were signs of a diurnal cycle. A corresponding minimum in the CO_2 concentrations above the sea was also observed (as well as the terrestrial sink).

Carbon dioxide measurements at Sammaltunturi give a reliable estimate of tropospheric background concentration influenced by both continental and marine sinks and sources. In the future results will be utilized in the construction of a transport model, where knowledge of the extent of the source area and location of sources within are of great importance. Criteria for the data classification according to the strength of local influence will also be developed.

5. Acknowledgements

We thank Dr. Aki Virkkula for useful discussions, Dr. Andreas Stohl for the program code for trajectory analysis and two anonymous reviewers for useful comments. Financial support from the Academy of Finland and co-operation with the Finnish Forest Research Institute, Pallas-Ounastunturi National Park, are gratefully acknowledged.

REFERENCES

Ahonen, T., Aalto, P., Rannik, U., Kulmala, M., Nilsson, E. D., Palmroth, S., Ylitalo, H. and Hari, P. 1997. Variations and vertical profiles of trace gas and aerosol concentrations and CO_2 exchange in Eastern Lapland. *Atmos. Environ.* **31**, 3351–3362.

Andres, R. J., Marland, G., Fung, I. and Matthews, E. 1996. A $1^\circ \times 1^\circ$ distribution of carbon dioxide emissions from fossil fuel consumption and cement manufacture, 1950–1990. *Global Biogeochem. Cycles* **10**, 419–429.

Andres, R. J., Fielding, D. J., Marland, G., Boden, T. A., Kumar, N. and Kearney, A. T. 1999. Carbon dioxide emissions from fossil-fuel use, 1751–1950. *Tellus* **51B**, 759–765.

Aurela, M., Laurila, T. and Tuovinen, J-P. 2001. Seasonal CO_2 balances of a subarctic mire. *J. Geophys. Res.* **106**, 1623–1637.

Bakwin, P. S., Tans, P. P., Hurst, D. F. and Zhao, G. 1998. Measurements of carbon dioxide on very tall towers: results of the NOAA/CMDL program. *Tellus* **50B**, 401–415.

Bonan, G. B. Chapin, F. S. and Thompson, S. L. 1995. Boreal forest and tundra ecosystems as components of the climate system. *Climatic Change* **29**, 145–167.

Bousquet, P. Peylin, P. Ciais, P. Ramonet, M. and Monfray, P. 1999. Inverse modeling of annual atmospheric CO_2 sources and sinks. Part 2: Sensitivity study. *J. Geophys. Res.* **104**, 26,179–26,193.

Colombo, T., Santaguida, R., Capasso, A., Calzolari, F., Evangelisti, F. and Bonasoni, P. 2000. Biospheric influence on carbon dioxide measurements in Italy. *Atmos. Environ.* **34**, 4963–4969.

Conway, T. J., Tans, P. P., Waterman, L. S., Thoning, K. W., Kitzis, D. R., Masarie, K. A. and Zhang, N. 1994. Evidence for interannual variability of the carbon cycle from the National Oceanic and Atmospheric Administration/Climate Monitoring and Diagnostics Laboratory Global Air Sampling Network. *J. Geophys. Res.* **99**, 22,831–22,855.

Cooke, W. F. and Wilson, J. J. N. 1996. A global black carbon aerosol model. *J. Geophys. Res.* **101**, 19,395–19,409.

Ciais, P., Tans, P. P., Trolier, M., White, J. W. C. and Francey, R. J. 1995. A large northern hemisphere terrestrial sink indicated by the $^{13}C/^{12}C$ ratio of atmospheric CO_2. *Science* **269**, 1098–1101.

Engardt, M. and Holmén, K. 1999. Model simulations of anthropogenic CO_2 transport to an Arctic monitoring station during winter. *Tellus* **51B**, 194–209.

Fan, S., Gloor, M., Mahlman, J., Pacala, S., Sarmiento, J., Takahashi, T. and Tans, P. 1998. A large terrestrial carbon sink in north America implied by atmospehric and oceanic carbon dioxide data and models. *Science* **282**, 442–446.

Gloor, M., Fan, S. Pacala, S. Sarmiento, J. and Ramonet, M. 1999. A model-based evaluation of inversions of atmospheric transport, using annual mean mixing ratios, as a tool to monitor fluxes of nonreactive trace substances like CO_2 on a continental scale. *J. Geophys. Res.* **104**, 14,245–14,260.

Hatakka, J., Trivett, N., Paatero, J., Laurila, T. and Viisanen, Y. 2001. *GAW research programme at Pallas, Finland.* WMO Report (in press).

Intergovernmental Panel on Climate Change (IPCC). 2001. *Climate change 2001: the scientific basis*, Cambridge University Press, New York.

Kahaner, D., Moler, C. and Nash, S. 1989. *Numerical methods and software*, Prentice-Hall Inc., Englewood Cliffs, NJ.

Keeling, C. D. 1995. Interannual extremes in the rate of rise of atmospheric carbon dioxide since 1980. *Nature* **375**, 666–670.

Laurila, T. and Hakola, H. 1996. Seasonal cycle of C_2–C_5 hydrocarbons over the Baltic Sea and Northern Finland. *Atmos. Environ.* **30**, 1597–1607.

Laurila, T. 1999. Observational study of transport and photochemical formation of ozone over Northern Europe. *J. Geophys. Res.* **104**, 26,235–26,243.

Laurila, T., Soegaard, H., Lloyd, C. R., Aurela, M., Tuovinen, J-P. and Nordstroem, C. 2001. Seasonal variations of net CO_2 exchange in European Arctic ecosystems. *Theor. Appl. Climatol.* **70**, 183–201.

Levin, I., Graul, R. and Trivett, N. B. A. 1995. Long-term observations of atmospheric CO_2 and carbon isotopes at continental sites in Germany. *Tellus* **47B**, 23–34.

Logan, J. A. 1985. Tropospheric ozone: seasonal behavior, trends, and anthropogenic influence. *J. Geophys. Res.* **90**, 10,463–10,482.

Markkanen, T., Rannik, U., Keronen, P., Suni, T. and Vesala, T. 2000. Eddy covariance fluxes over a boreal Scots pine forest. *Boreal Environ. Res.* **6**, 65–78.

Olson, M. P., Oikawa, K. K. and Macfee, A. W. 1978. *A trajectory model applied to the long range transport of air pollutants: a technical description and some model comparisons.* Report LRTAP 78–4, Atmospheric Environment Service, Downsview, Ontario, Canada.

Paatero, J. and Hatakka, J. 2000. Source areas of airborne 7Be and 210Pb measured in Northern Finland. *Health Phys.* **79**, 691–696.

Paatero, J., Hatakka, J. and Viisanen, Y. 1999. Meteorological aspects of radon-222 concentrations in the air at the Pallas GAW station, northern Finland. *J. Aerosol Sci.* **30**, S603–S604.

Pöllänen, R., Valkama, I. and Toivonen, H. 1997. Transport of radioactive particles from the Chernobyl accident. *Atmos. Environ.* **31**, 3575–2590.

Rahn, K. A., Joranger, E., Semb, A. and Conway, T. J. 1980. High winter concentrations of SO_2 in the Norwegian Arctic and transport from Eurasia. *Nature* **287**, 824–826.

Rinne, J., Tuovinen, J.-P., Laurila, T., Hakola, H., Aurela, M. and Hypen, H. 2000. Measurements of hydrocarbon fluxes by a gradient method above a northern boreal forest. *Agric. Forest Meteorol.* **102**, 25–37.

Rummukainen, M., Laurila, T. and Kivi, R. 1996. Yearly cycle of lower tropospheric ozone at the arctic circle. *Atmos. Environ.* **30**, 1875–1885.

Seibert, P., Kromb-Kolb, H., Baltensperger, U., Jost, D. T., Schwikowski, M., Kasper, A. and Puxbaum, H. 1994. Trajectory analysis of aerosol measurements at high alpine sites. In: *Transport and transformation of pollutants in the troposphere* (eds. P. M. Borrell, P. Borrell, T. Cvitas and W. Seiler), Academic Publishing, Den Haag, 689–693.

Seinfeld, J. H. and Pandis, S. N. 1998. *Atmospheric chemistry and physics: from air pollution to climate change*. Wiley & Sons, New York.

Stohl, A. 1996. Trajectory statistics — a new method to establish source–receptor relationships of air pollutants and its application to the transport of particulate sulfate in Europe. *Atmos. Environ.* **30**, 579–587.

Stohl, A. 1998. Computation, accuracy and applications of trajectories — s review and bibliography. *Atmos. Environ.* **32**, 947–966.

Tans, P. P., Thoning, K. W., Elliot, W. P. and Conway, T. J. 1989. *Background atmospheric CO_2 patterns from weekly flask samples at Barrow, Alaska: optimal signal recovery and error estimates.* NOAA Tech. Memo. (ERL-ARL-173), Environmental Research Laboratory, Boulder, Colorado, 131 pp.

Tuovinen, J.-P., Laurila, T., Lättilä, H., Ryaboshapko, A., Brukhanov, P. and Korolev, S. 1993. Impact of the sulphur dioxide sources in the Kola Peninsula on air quality in northernmost Europe. *Atmos. Environ.* **27A**, 1379–1395.

Virkkula, A., Hillamo, R. E., Kerminen, V-M. and Stohl, A. 1998. The influence of Kola Peninsula, continental European and marine sources on the number concentrations and scattering coefficients of the atmospheric aerosol in Finnish Lapland. *Boreal Environ. Res.* **2**, 317–336.